Normal and Abnormal Pulmonary Ventilation: Visualization at Hyperpolarized He-3 MR Imaging[1]

Hans-Ulrich Kauczor, MD
Dirk Hofmann, MS
Karl-Friedrich Kreitner, MD
Helge Nilgens, PhD
Reinhard Surkau, PhD
Werner Heil, PhD
Andreas Potthast, MS
Michael V. Knopp, MD
Ernst W. Otten, PhD
Manfred Thelen, MD

To assess the feasibility of helium-3 magnetic resonance (MR) imaging with a three-dimensional fast low-angle shot (FLASH) sequence, He-3 gas (volume, 300 mL; pressure, 3×10^5 Pa; polarized up to 45% by means of optimal pumping) was inhaled by five healthy volunteers and five patients with pulmonary diseases. All breath-hold examinations (22–42 seconds) were completed successfully. Normal ventilation was depicted with homogeneous high signal intensity, lesions were depicted as causing defects, and obstructive lung disease was depicted with severely inhomogeneous signal intensity.

Index terms: Lung, MR, 60.12143 • Magnetic resonance (MR), contrast enhancement, 60.12143 • Magnetic resonance (MR), nuclei other than H, 60.12147

Radiology 1996; 201:564–568

RECENTLY, use of hyperpolarized noble gases, such as xenon-129 or helium-3, has been proposed in magnetic resonance (MR) imaging examinations because such gases open a new field of promising possibilities to enhance signal (1–3). In these examinations, the source of the MR signal is the large nonequilibrium polarization in the nuclei of the hyperpolarized noble gases. Nuclear spin polarization is achieved by means of optical pumping techniques. In noble gases, such as He-3, optical pumping makes hyperpolarization over ordinary Boltzman equilibrium possible (4), and the polarization reaches the order of unity. In comparison, in a normal magnetic field (1.5 T) the polarization of protons is as small as 5×10^{-6}. The high spin density of the He-3 gas compensates for the otherwise very low signal of He-3, which is caused by the low density of the gas. Subsequently, a high degree of polarization is essential to allow detection of an adequate MR signal. Helium gas can be inhaled in considerable amounts and concentrations (80% helium, 20% oxygen) without risk, on the basis of findings in deep sea diving and special lung function tests (measurement of the residual volume). After hyperpolarized He-3 gas is inhaled, the airways and alveolar air spaces can be visualized with a strong signal intensity, as has been demonstrated in the guinea pig lung (3) and in preliminary studies in humans (5–7). Findings in these studies suggest that He-3 MR imaging can depict lung morphology and can help assessment of pulmonary ventilation. The purpose of our study was to prove the feasibility of MR imaging with hyperpolarized He-3 gas and to demonstrate the He-3 MR imaging findings of normal ventilation in healthy volunteers and of ventilatory abnormalities in patients with different pulmonary diseases.

Materials and Methods

Hyperpolarization of He-3 gas is achieved by means of direct optical pumping of the He-3 gas from its metastable $1s2s\,^3S_1$ state populated to a low-pressure (10^2 Pa) discharge. Multiple metastability exchange collisions to the nuclei of the ground- state atoms transfer the polarization with a large cross section (4). With use of high laser power and high pumping volumes, high production rates are obtained. We used an arc-lamp–pumped laser composed of $La_{0.85}Nd_{0.15}MgAl_{11}O_{13}$ (LNA laser), which delivers about 8 W at the desired wavelength of 1.08 μm. This equipment is able to polarize about 6 L of gas up to a polarization of about 65% within 30 seconds (8). This corresponds to a production rate of approximately 6×10^{18} polarized spins per second. Achievement of high spin densities up to 45% is a prerequisite for the clinical application of He-3 MR imaging (5). Since the polarization level could not be measured for each sample used in our study, spot checks were performed and revealed polarization levels between 35% and 45%. A convenient pressure for the hyperpolarized gas of $1–5 \times 10^5$ Pa is achieved with use of a specially designed nonmagnetic compression system without a major loss in polarization (9). Within 2 hours, 300 mL of the compressed hyperpolarized gas was filled into a glass cell at a pressure of 3×10^5 Pa. To facilitate storage, transport, and handling, achievement of long relaxation times in the hyperpolarized gas within the glass cell is indispensable. Relaxation of the hyperpolarized gas can be lost owing to interactions with the wall of the glass cell, penetration through the glass cell, or the presence of oxygen. Thus, filling is performed under vacuum conditions, and a special internally coated glass (Supremax; Schott Glaswerke, Mainz, Germany) is used to achieve long relaxation times with a T1 of up to 100 hours (10). These glass cells are equipped with a glass stopcock to give off the compressed hyperpolarized gas. After use, the glass cell can be refilled easily and reused. To transport the glass cells from the filling site to the MR imaging unit, they were manually placed in the center of a dedicated small holding field of 0.3 mT. For the imaging examinations, the glass cells containing the hyperpolarized He-3 gas were manually carried from the holding field to the magnet and handed over to the subject in its center within less than 5 seconds to avoid any loss of polarization caused by the field gradients in the stray field zone.

All imaging examinations were performed on a 1.5-T whole-body MR imager (Magnetom Vision; Siemens Medical Systems, Erlangen, Germany). A dedicated transmit-receive Helmholtz coil operating at 48.44 MHz was constructed for He-3 imaging. This coil has a circular shape with an outer diameter of 31.5 cm and a twin-ring design with a variable distance between the two rings of 20.0–25.5 cm. At MR imaging, the volunteer's or patient's chest was positioned between the anterior and posterior rings of the Helmholtz coil. At deep inspiration, the anterior ring of this flat nonflexible coil was lowered until it reached the anterior chest wall. Exact positioning is essential since scout views for planning are not ob-

[1] From the Department of Radiology (H.U.K., K.F.K., H.N., M.T.) and the Institute of Physics (D.H., R.S., W.H., E.W.O.), Johannes Gutenberg-Universität Mainz, Langenbeckstr 1, 55131 Mainz, Germany; Siemens Medical Systems, Erlangen, Germany (A.P.); and the Department of Oncologic Diagnostics and Therapy, German Cancer Research Center, Heidelberg, Germany (M.V.K.). Received April 24, 1996; revision requested June 3; revision received June 24; accepted July 1. **Address reprint requests to** H.U.K.

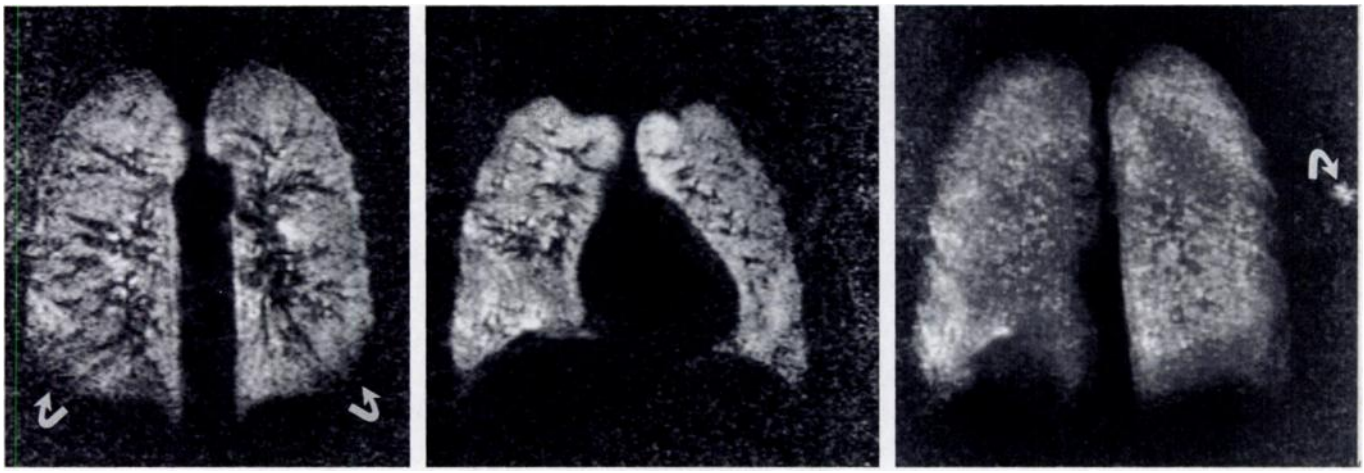

a. b. c.

Figure 1. He-3 MR images were obtained after inhalation of hyperpolarized He-3 gas in a 33-year-old healthy volunteer (nonsmoker). **(a, b)** Coronal three-dimensional FLASH images show homogeneous ventilation of the **(a)** posterior and **(b)** anterior upper and lower lungs depicted with high signal intensity. The pulmonary vessels appear as structures without signal intensity. Note the basal curvilinear areas (arrows in **a**) that are without signal intensity owing to limitations in the experimental circular Helmholtz coil. **(c)** Maximum-intensity-projection image illustrates the rather homogeneous ventilation in all lungs. Note a hyperintense spot on the left, which represents residual He-3 gas within the glass cell (arrow).

tained. One capacitor (22 pf) was attached to each loop. One serial (4.5–51.0 pf) and one parallel (5–25 pf) variable capacitor was applied to tune and match. The coil was manually tuned with the subject in the center of the magnet. At imaging, the broadband system of the regular spectroscopic accessory of the MR imaging system was applied. The gradient strengths were adjusted to the gyromagnetic ratio of He-3. No additional hardware changes were necessary in our commercially available MR imaging unit.

Prior to the imaging examination itself, the inhalation procedure was rehearsed several times. During rehearsal, a glass cell identical to the specially designed glass cell for the hyperpolarized He-3 gas was filled with ordinary (nonpolarized) He-4 (volume, 300 mL; pressure, $\approx 3 \times 10^5$ Pa) and handed to the subject within the magnet. Breathing through the nose was inhibited by applying a nose clamp. The inhalation procedure started with the subject taking two deep breaths of ordinary air. Then the subject took two deep breaths of ordinary He-4 gas that was supplied from a special reservoir. Immediately afterward, the subject switched to the glass cell, took the tip into his or her mouth, opened the glass stopcock, inhaled the He-4 gas, and held his or her breath in maximum inspiration. As a guideline for the breath-hold period requested, the imaging sequence was started simultaneously. Since nonpolarized He-4 was used at this time, no signal was obtained. If the volunteer or patient was not capable of holding his or her breath long enough, the sequence was adapted accordingly. When the subject was familiar with the inhalation procedure, the sample containing the hyperpolarized He-3 gas was rapidly carried from the holding field to the magnet and handed over to the subject in its center. With this sample positioned in the center of the coil, the larmor frequency of helium was adjusted again (transmitter amplitude, 0.01 V). The whole inhalation procedure was repeated and, immediately after the inhalation of the hyperpolarized He-3 gas, the imaging sequence was started.

He-3 MR imaging examinations were performed in five healthy volunteers (four men and one woman, aged 25–33 years [mean, 29 years]). All were nonsmokers. The fast low-angle shot (FLASH) sequence was applied (repetition time [msec]/echo time [msec] = 11.8/5; with total receiver gain of 85 dB, matrix size of 144 × 256, and field of view of 350 mm). The transmitter amplitude varied between 5 and 7 V, depending on body weight and chest size. On the basis of findings in prior experiments with hyperbaric nonpolarized He-3 and a large saline-filled phantom that mimicked a human chest, this transmit voltage corresponded to a flip angle of less than 5°. One slab in the coronal orientation with a thickness of 170 mm and 24 partitions, which resulted in an effective section thickness of 7.08 mm, was acquired within 42 seconds, which represented the breath-hold period necessary.

He-3 MR imaging examinations were also performed in five patients (four men and one woman, aged 29–60 years [mean, 48.6 years]). They experienced chronic obstructive pulmonary disease and emphysema ($n = 1$), chronic obstructive pulmonary disease and bronchogenic carcinoma ($n = 1$), unilateral destroyed lung with cavitation ($n = 1$), fibrosis ($n = 1$), and bihilar and mediastinal lymphadenopathy in Hodgkin disease ($n = 1$). The two patients with chronic obstructive pulmonary disease were smokers, and the other three patients were nonsmokers. Informed consent was obtained from all patients after the procedure had been fully explained. The three-dimensional FLASH sequence was modified to reduce the acquisition time according to the ability of the individual patient to hold his or her breath. The following sequence was used: 11.8/5; transmitter amplitude, 5–7 V (depending on body weight and chest size, which corresponded to a flip angle of less than 5°); total receiver gain, 85 dB; matrix, 144 × 256; field of view, 350 mm; and acquisition in the coronal plane. In four patients, the slab thickness was 150 mm with 18 partitions, which resulted in an effective section thickness of 8.33 mm and an acquisition time of 32 seconds. In one patient, the matrix size was set to 128 × 256, the slab thickness was reduced to 140 mm, and 14 partitions were chosen, which resulted in an effective section thickness of 10 mm to reduce the breath-hold period to 22 seconds. Maximum intensity projections were obtained from the sections that depicted signal intensity in all examinations.

The MR imaging examination was successful if the hyperpolarized He-3 gas was detected within the lungs as an area with high signal intensity. Source images and maximum intensity projections were assessed visually: The signal intensity within the trachea; the main stem bronchi; and the upper, lower, anterior, and posterior lungs was rated on

a 3-point scale as none, hypointense, or hyperintense. Additionally, the presence, severity (mild, moderate, or severe), and localization of signal intensity inhomogeneities were noted. In patients, the presence of localized signal intensity defects or inhomogeneities was correlated with the underlying disorders.

Results

All 10 MR imaging examinations were completed successfully. The hyperpolarized He-3 gas was depicted as a hyperintense area within the airways and the pulmonary air spaces in all volunteers and patients (Fig 1).

The trachea was hyperintense in seven cases and hypointense in three. Nineteen of 20 main stem bronchi were visualized; 13 were hyperintense and six were hypointense.

In four volunteers there was no difference in signal intensity between the upper and lower lungs (Fig 1). The lungs in three volunteers were hyperintense and in one were hypointense. In one volunteer, the lower lungs were predominantly hyperintense and the upper lungs were predominantly hypointense. In all volunteers, the posterior lungs were hyperintense. The anterior lungs were hyperintense in three volunteers (Fig 1b) and were hypointense in two. A slight decrease in signal intensity toward the central lungs—with increasing distance from the twin-ring coil system—was depicted in two volunteers. In two volunteers, peripheral wedge- and curve-shaped hypointense areas (in the lower lateral lungs) were observed (Fig 1a). Mild signal intensity inhomogeneities were depicted in two volunteers. The maximum-intensity-projection images confirmed the complete and almost homogeneous ventilation in the lungs (Fig 1c). They resembled ventilation scintigraphy images.

In patients, the lung parenchyma that was not involved with focal disease was hyperintense in the upper (n = 4), lower (n = 5), anterior (n = 4), and posterior (n = 5) lungs. In the other two cases, such lung parenchyma was hypointense. Bronchogenic carcinoma (Fig 2), bihilar lymphadenopathy, and the unilaterally destroyed lung with cavitation (Fig 3) resulted in large signal intensity defects. These lesions were associated with areas of low or no signal intensity in the adjacent or more peripheral lungs. These large defects were illustrated clearly on the maximum-intensity-projection images. On the images obtained in the two patients with chronic obstructive pulmonary disease (both of whom were smokers), severe localized and diffuse inhomogeneities in signal intensity were detected (Fig 4a). The maximum-intensity-projection images demonstrated severe signal intensity inhomogeneities throughout the lungs, giving them a bubblelike appearance (Fig 4b). Localized hyperintense areas were found directly adjacent to hypointense areas. Hypointense areas were seen most often in the periphery of the lungs, with a wedge-shaped configuration demonstrated equally well on the source and maximum-intensity-projection images. In the patient with mild fibrosis due to systemic sclerosis, we observed only a few linear defects in the lower lungs (Fig 5a), which corresponded to the more severe computed tomographic (CT) findings (reticular translobular lines and ground glass opacity) (Fig 5b).

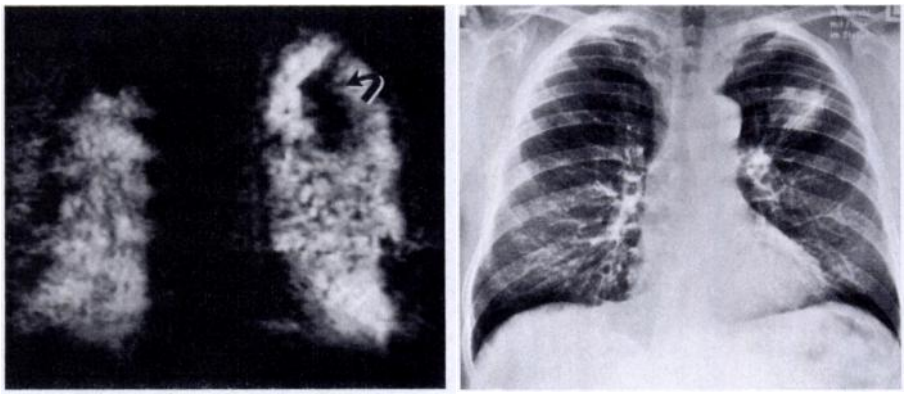

a. b.

Figure 2. He-3 MR image was obtained in a 50-year-old patient with bronchogenic carcinoma and chronic obstructive pulmonary disease. **(a)** Coronal three-dimensional FLASH image shows a large area with no signal intensity in the posterior segment of the left upper lobe that was caused by the tumor and which compromised ventilation in the adjacent air spaces (arrow), as well as peripheral areas with signal intensity defects that represent hypoventilation. **(b)** Corresponding chest radiograph shows the tumor in the left upper lobe.

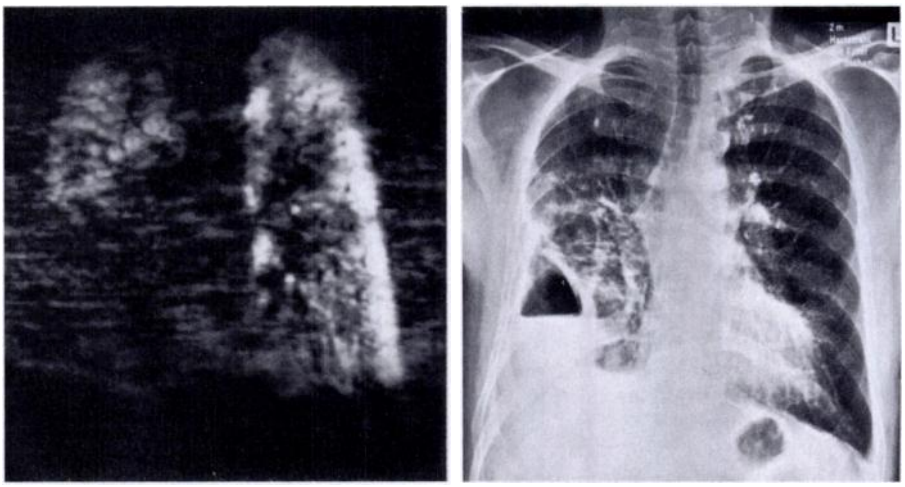

a. b.

Figure 3. He-3 MR image was obtained in a 52-year-old patient with a destroyed right lung and cavitation in the right lower lobe. **(a)** Coronal three-dimensional FLASH image shows a large ventilatory defect in the right lower lobe. **(b)** Corresponding chest radiograph shows cavitation in the right lower lobe.

Discussion

In this study, we demonstrated the technical feasibility of performing MR imaging after inhalation of hyperpolarized He-3 gas in healthy volunteers and patients with pulmonary diseases. At He-3 MR imaging, the airways and ventilated air spaces are constantly shown as hyperintense areas.

Visualization of the trachea and main stem bronchi with high signal intensity confirmed the inspiratory breath hold immediately after inhalation of the hyperpolarized He-3 gas in nearly all cases. Depiction of the main stem bronchi depends on size, signal intensity, and section thickness. The technique is not currently suited to help assess possible alterations in the central airways

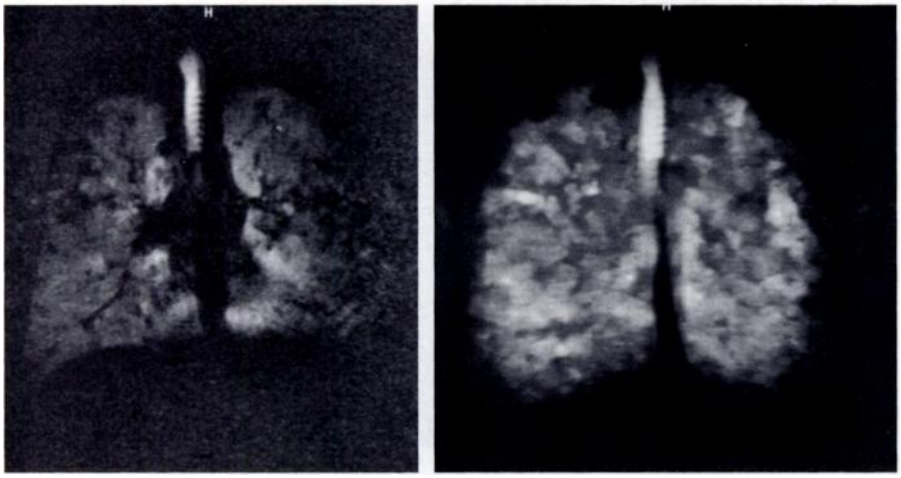

a. b.

Figure 4. He-3 MR image was obtained in a 49-year-old patient with chronic obstructive pulmonary disease and emphysema. **(a)** Coronal three-dimensional FLASH image shows marked signal intensity inhomogeneities throughout the lungs. **(b)** Maximum-intensity-projection image illustrates massive alterations in pulmonary architecture and ventilation and depicts the lungs with a bubblelike appearance. Note the high signal intensity in the trachea.

because the sections are rather thick and the spatial resolution is limited. Conventional proton MR imaging is superior to He-3 MR imaging in the assessment of central airways. The lobar bronchi cannot be delineated, probably owing to superimposition of the adjacent ventilated hyperintense parenchyma. The patency of the airways, however, can be evaluated indirectly by demonstrating hyperintense areas in the corresponding peripheral areas.

The He-3 MR images obtained in most volunteers depicted a rather homogeneous distribution of the inhaled He-3 gas within the air spaces. Direct visualization of the air spaces at He-3 MR imaging represents an important new development and is a considerable advantage compared with findings at conventional proton MR imaging. We found only a few small peripheral wedge-shaped areas with less signal intensity. In healthy and nonsmoking volunteers, we interpreted the presence of these areas as indicating insufficient inspiration of the He-3 gas. In general, the amount of He-3 gas (300 mL) provided seems to be sufficient to visualize all ventilated air spaces if the gas is properly inhaled. This volume is much less than that used in other studies in which a lower polarization level (750 mL) was used (7). In He-3 MR imaging the lower and posterior lungs—which are known to be preferentially ventilated—constantly exhibited high signal intensity, whereas the upper and anterior portions exhibited low signal intensity in a few cases. These findings may represent local hypoventilation in the supine position. Additionally, differences in signal intensity between the lungs adjacent to the two rings of the coil and the central lungs can be partially attributed to the experimental design of the Helmholtz coil, which does not completely compensate for the slight signal losses that occur with increasing distance from the coil. Compared with use of a single surface coil (7), use of the twin-ring system of the Helmholtz coil results in better homogeneity, and there is no obvious penetration or receptivity limit. Owing to this design, the slight signal intensity falloff in the central lungs did not have to be corrected before maximum intensity projection to avoid a bias with regard to the central sections. The diameter of the coil and the subsequent limitations of the field of view are also responsible for curve-shaped signal intensity losses in the peripheral areas of the lower lungs (Fig 1a).

Focal lesions, such as bronchogenic carcinoma or enlarged hilar lymph nodes, lead to ventilation defects in patients that are easily appreciated at He-3 MR imaging. Interestingly, the ventilation defects are larger than the lesions themselves at chest radiography or CT (Figs 2, 3). Thus, these lesions are associated with adjacent ventilation disturbances that are detectable at He-3 MR imaging. The most surprising observations are made in smokers with known chronic obstructive pulmonary disease. The marked signal intensity inhomogeneities are a clear indication of the severe abnormalities of pulmonary ventilation in these patients. It is well known that smoking and chronic obstructive pulmonary disease result in chronic inflammation, bronchial hyperreagibility, and expiratory airflow obstruction. Since He-3 MR imaging represents an inspiratory single-breath technique, these signal intensity inhomogeneities originate from airway alterations that change the distribution of air during inspiration. Areas or even compartments with different ventilatory levels are recognized. Some areas seem to be hyperventilated because they exhibit a very high signal intensity that is even higher than that depicted on images obtained in healthy volunteers. Other areas have low or no signal intensity, which indicates local hypoventilation. Until now, the technique itself did not provide any information about the possible existence of expiratory obstruction (air trapping). In our patients, hyperventilated and hypoventilated areas were equally distributed throughout the lungs without any predominance in central or peripheral regions or any other location. On the basis of our preliminary experience, we believe He-3 MR imaging can help visualize profound changes in pulmonary ventilation in smokers and patients with chronic obstructive pulmonary disease with high reliability and accuracy. Our data provide new topographic and functional insights into pulmonary pathophysiology. In the clinical context, this new modality may help assessment of patients with emphysema and chronic obstructive pulmonary disease who undergo thoracic surgery to treat malignant disease or of candidates prior to volume-reduction surgery or lung transplantation.

Although the observation of severe signal intensity inhomogeneities is exciting, we have to keep in mind that we visualized the inspiratory distribution of helium and not ordinary air. Helium has some distinct differences: small atom size, low atomic weight and viscosity, fast penetration and diffusion into the air spaces, and negligible tissue resorption. The possible influences of these properties on sequence design and signal-to-noise ratios and their clinical importance necessitates further investigation. Additionally, the presence and severity of local signal intensity losses due to the contact between oxygen and hyperpolarized He-3 gas and their importance in the interpretation of imaging findings warrant further studies. It is known that the direct contact of oxygen, as present in ordinary air, and hyperpolarized He-3 gas results in a drop in the longitudinal relaxation time of hyperpolarized He-3 to about 10 seconds (11). Since the MR acquisition takes 30–40 seconds, we intended to avoid immediate contact of hyperpolarized He-3 gas and oxygen during inhalation of the sample. Subsequently, our inhalation procedure included two deep breaths of ordinary helium to wash out ordinary air and its oxygen from the lungs. This procedure was successfully implemented in the

inhalation procedure, and the longitudinal relaxation time of hyperpolarized He-3 was prolonged to approximately 35 seconds as we have confirmed with our own measurements (unpublished results).

It should be noted that every excitation depletes polarization from the hyperpolarized He-3 sample. The polarization cannot be recovered because the nuclear polarization is far above the Boltzman equilibrium state. Consequently, only one acquisition is possible with each He-3 sample inhaled. Thus, all examinations are performed without acquisition of scout views and in a single breath hold. Use of small flip angles is mandatory in He-3 MR imaging pulse sequences to ensure a relatively constant magnetization during the acquisition period. The three-dimensional FLASH sequence we applied is well suited for He-3 MR imaging. It provides a breath-hold acquisition, a small flip angle (<5°), T1 weighting, good signal-to-noise ratio, and full postprocessing capabilities. Compared with results achieved with the two-dimensional FLASH sequence (5), image quality is improved. Nevertheless, further development of more efficient pulse sequences is warranted.

He-3 MR imaging is a new, promising imaging modality to help visualize and assess pulmonary ventilation. It will help provide further insights into the pathophysiology of breathing, and it may challenge ventilation scintigraphy in the preoperative work-up of patients with pulmonary disease. Since only a few accessory tools are needed to perform He-3 MR imaging—with the exception of a dedicated coil—this technique could become widely available within a short time. Quantities of He-3 are limited because the gas is generated by means of tritium decay. Further developments such as improvement in sequences, use of smaller volumes of He-3, and recycling of He-3 are under way.

At the moment the cost for one sample of hyperpolarized He-3 is about $300, but this cost will be reduced with increasing demand. More experience is indispensable to evaluate the characteristics and potential of He-3 MR imaging under clinical conditions. ■

Acknowledgments: We appreciate the continuous support of Michael Deimling, PhD, and Wilhelm Dürr, PhD, from Siemens Medical Systems, Erlangen, Germany. We thank Schott Glaswerke (Mainz, Germany) for developing the coated glass cells. We are grateful to Michèle Leduc, PhD, (Laboratoire Kastler-Brossel, École Normale Supérieure, Paris, France) for her expertise in the polarization process. We thank Peter Bachert, PhD, Michael Bock, PhD, and Lothar Schad, PhD, from the Department of Medical Physics of the German Cancer Research Center (Heidelberg, Germany) for their cooperation.

References

1. Albert MS, Cates GD, Driehuys B, et al. Biological magnetic resonance imaging using laser-polarized ^{129}Xe. Nature 1994; 370:199–201.
2. Albert MS, Schepkin VD, Budinger TF. Measurement of ^{129}Xe T1 in blood to explore the feasibility of hyperpolarized ^{129}Xe MRI. J Comput Assist Tomogr 1995; 19:975–978.
3. Black RD, Middleton HL, Cates GD, et al. In vivo He-3 MR images of guinea pig lungs. Radiology 1996; 199:867–890.
4. Eckert G, Heil W, Meyerhoff M, et al. A dense polarized ^3He target based on compression of optically pumped gas. Nucl Instr Methods Phys Res 1992; A320:53–65.
5. Ebert M, Grossmann T, Heil W, et al. Nuclear magnetic resonance imaging on humans using hyperpolarized ^3He. Lancet 1996; 347:1297–1299.
6. Bachert P, Schad L, Bock M, et al. Nuclear magnetic resonance imaging of airways in humans with use of hyperpolarized ^3He. Magn Reson Med 1996; 36:192–196.
7. MacFall JR, Charles HC, Black RD, et al. Human lung air spaces: potential for MR imaging with hyperpolarized He-3. Radiology 1996; 200:553–558.
8. Heil W, Surkau R. Development of a dense polarized ^3He spin filter based on compression of optically pumped gas. J Neutron Res (in press).
9. Becker J, Heil W, Krug B, et al. Study of mechanical compression of spin-polarized ^3He gas. Nucl Instr Methods Phys Res 1994; A346:45–51.
10. Heil W, Humblot H, Otten E, Schäfer M, Surkau R, Leduc M. Very long nuclear relaxation times of spin polarized helium 3 in metal coated cells. Phys Lett 1995; A201: 337–343.
11. Saam B, Happer W, Middleton H. Nuclear relaxation of ^3He in the presence of O_2. Phys Rev 1995; A52:862–865.

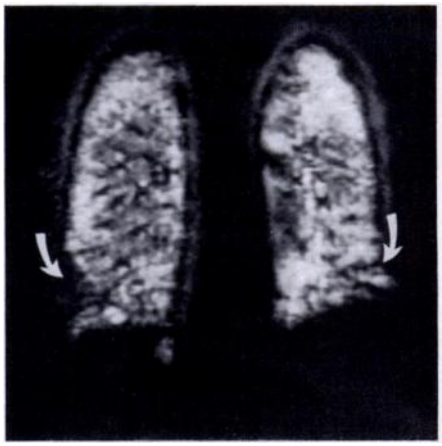

a.

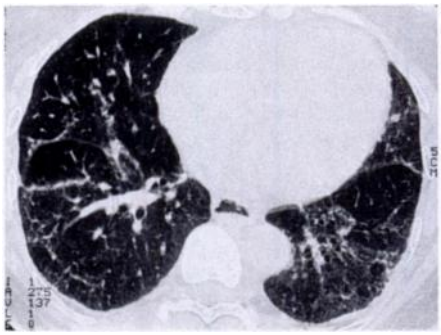

b.

Figure 5. He-3 MR image was obtained in a 59-year-old patient with fibrosis due to systemic sclerosis. **(a)** Coronal three-dimensional FLASH image shows only minor ventilatory compromise in both lower lobes (arrows). **(b)** Corresponding thin-section CT scan depicts reticular translobular lines and ground glass opacity in both lower lobes.